



**Acoustics'08  
Paris**  
June 29-July 4, 2008  
[www.acoustics08-paris.org](http://www.acoustics08-paris.org)

## Computer learning method for scattering junction identification

Adam Kestian<sup>a</sup> and Agnieszka Roginska<sup>b</sup>

<sup>a</sup>New York University, 77 Park Ave., apt 1214, Hoboken, NJ 07030, USA

<sup>b</sup>New York University, 35 West Fourth St., Room 777, New York, NY 10012, USA  
apk240@nyu.edu

Acoustic reflectometry is a non-invasive, time-domain method that is used to identify the geometry of an acoustical space. A sound pulse is injected into a space and the resulting impulse response details particular changes of impedance, which is a result of a cross-sectional area change or an elbow/T-intersection. Each cause of reflection, known as a scattering junction, has a distinct reflection contour. Previous works were able to identify these scattering junctions via algorithms that attempt to extract particular contours from the impulse response. In the present study, the prominent reflections of the space are observed, isolated, and then compared to a training database of all possible scattering junctions. This method eliminates the necessity to create a contour identification algorithm, as scattering junctions are defined based on its most similar neighbors in the training database. Results suggest that this computer-learning algorithm can successfully identify reflection contours of a space with varying cross-sectional areas from those that were stored in the training database, which suggests that this method could be a more efficient and versatile alternative to previous identification processes.

## 1 Introduction

Acoustic Pulse Reflectometry (APR) provides the ability to obtain numerous features about a cavity through its impulse response. These features can include the length, cross-sectional area, and scattering junction of each segment of the cavity. Other works [1] have also identified leaks in the cavity, which is typically of note when investigating acoustic instruments. The specific details of the cavity can be obtained from the temporal cues, the magnitude of each reflection, and its contour.

APR was first developed as a seismological technique for observations regarding the earth's crust [2] and the geometry of the human airway [3] [4]. Later works [5] introduced a similar apparatus to what is used in this study. This apparatus consists of an auxiliary source tube with microphone embedded in its wall part of the way down. The impulse response of the cavity was obtained by deconvolving the airway reflections with the shape of the input pulse.

Recent studies [5] [6] investigated more specialized cavities. One of the most noteworthy innovations of [6] was the inclusion of bifurcation identification. T-intersections could be correctly identified in a variety of configurations.

In most studies with APR, including [7] and this study, the examined cavities are typically composed of narrow, cylindrical objects. The most notable reason for examining such cavities is that sound propagates uniformly in a single direction in such narrow spaces. This planar propagation leads to a more simplistic reconstruction task where the object is only observed in a single dimension. This is quite different than the propagation of non-planar waves. Non-planar waves propagate three-dimensionally. The more complex the impulse response becomes, the more difficult it becomes to isolate and identify specific scattering junctions. Any frequency whose wavelength is greater than the cross-sectional area of the tube will propagate in this fashion. Considering the largest tube used in testing is 1.27 cm, frequencies greater than 15.7 kHz may propagate in a non-planar manner.

Sound waves both reflect and transmit at any change of impedance. In the case of this specific test setup, the only instance of impedance change with planar waves is a change in cross-sectional area. The manner in which the cross-sectional area changes will determine the contour of the reflection. These causes of reflection are known as

scattering junctions. Previously [7], a scattering junction identification algorithm was devised to identify cross-sectional increase and decrease, L-intersection, and T-intersections. Based on this work, it is apparent that tubes of varying cross-sectional areas share similar scattering junction reflection contours. This goal of this research is to implement a computer-learning algorithm that can identify scattering junctions after a period of training. This will provide a more versatile identification method that can be used to reconstruct a more diverse collection of spaces, as APR's potential lies in the reconstruction of larger spaces including rooms and hallways.

It is worth noting that this study does not suggest that the computer-learning method chosen for this study (k-NN) is the best for such a task, rather it intends to show that it is possible to create an algorithm that can classify specific scattering junctions with varying cross-sectional areas.

## 2 Methodology

Fig. 1 provides the schematic setup for testing [8]. A sine sweep is produced by RME's Fireface 400 D/A A/D and then amplified by a Samson Servo 120 power amplifier. The signal was then emanated from an AuSIM's AuProbe loudspeaker. The loudspeaker is approximately 3 in. in diameter. This speaker is coupled to the .9525 cm diameter source tube via a 5 in. long funnel. The gradual reduction in diameter limits coupler reflections. If the diameter was cut abruptly at this point, a large discontinuity results at the join between the source tube and the object, leading to a large reflection at the start of the object reflections.

The source tube is necessary to provide a clean impulse response of the cavity without contamination from other influences. Portion  $l_1$  of the source tube it is there to provide adequate time for the microphone embedded to the source tube wall to record the object reflections without contamination from source reflections. The amount of time before contamination is  $2l_1/c$ . This means that  $l_1$  must be notably longer than the cavities being investigated. The entire impulse response is recorded, which will be of a longer duration than the time before contamination. This is necessary to avoid inaccurate results during deconvolution.

In this experiment, the length of  $l_1$  was 3.25 m long. It is not uncommon for  $l_1$  to range from three to five meters depending on the length of objects being tested. Obviously, the longer the test object, the more time that is necessary to

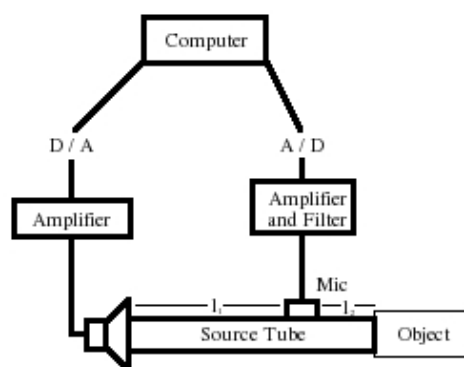


Fig. 1 - Testing apparatus

record all primary reflections, which also means a longer  $l_1$ . Eventually, a conflict results, as longer test objects require equally long length of  $l_1$  resulting in less accurate impulse response, as the impulse must travel a greater distance. It is possible to increase the amplitude of the pulse though there is a limit based on the point of speaker and amplifier distortion. Because the test objects used in this study were reasonably short, it was deemed unnecessary to implement strategies introduced in other studies [8].

The  $l_2$  is necessary to ensure that the reflections returning from the test object are reliable. This length separates the impulse emitted from the source and the primary reflection from the source tube. Because of  $l_2$ , it is ensured that the input pulse will be completely passed the microphone before the first reflections return. The length of  $l_2$  is 3.25 m long.

The test object is connected to the source tube via a simple tube coupler with a sharp attenuation or increase from source to test object. Like the tubes themselves, the couplers were made of copper. The sharp change from one cross-sectional area to the other is necessary to identify the corresponding change of cross-sectional area of the tubes themselves. A gradual reduction or increase would make it difficult to identify relevant scattering junctions.

While the source tube is necessary to obtain a proper impulse response of each cavity, the effects of the source tube must be removed from the impulse response of the test object. This can be accomplished by deconvolving the impulse response of the source tube with the impulse response of the source tube and cavity being investigated. Deconvolution is carried out in the frequency domain, which done by performing an FFT on both sets of impulse responses. Next, the two resulting signals are divided:

$$IR(w) = \frac{R(w)}{I(w) + q} \quad (1)$$

where  $w$  is the discrete angular frequency,  $R(w)$  is the FFT of the test cavity and  $I(w)$  is the FFT of the source tube. The signal that is retrieved from this complex division ( $IR(w)$ ) is then inverse Fourier Transformed in order obtain the impulse response in the time domain. A constraining factor of  $q$  is added to the input pulse in order to avoid division by zero, which can occur at higher

frequencies where the background noise can envelop the pulse. Effectively, the factor of  $q$  works as a low-pass filter.

The data was sampled at 44.1 kHz and then stored on a computer. A 25-second sine sweep was used as the test signal. This signal was repeated ten times and all of its repetitions were averaged in order to increase the signal-to-noise ratio<sup>1</sup>.

A thick copper cap was placed at the end of the final tube of each configuration, as well as the end of the source tube when its impulse response is taken. This type of cap was chosen because of their durability, uniformity, and strong reflectivity. Ideally, the entire impulse should be reflected perfectly with a minimal amount of attenuation.

The diameters of the tubes varied from lengths of .63 cm, .95 cm, and 1.27 cm. It was important that the scattering junctions, especially in the case with the T or L-intersections, that there were multiple trials with different diameter tube in order to make sure that its contour was consistent and not simply a result from a particular instance.

Figure 2 is the impulse response of one of the tube configurations used during the training portion of this study. In this particular case, a 1.27 diameter, 33 cm long bronze tube. The first two significant peaks signify the entrance and termination of that tube. The additional peaks at sample 240 and an even less strong peak at sample 332 are reflected test object, returned back towards the end of the test object, and then reflected towards the segmental border again. It is clear that these are in fact secondary reflections due to their periodicity, as their distance apart from each other closely mirrors the length of the test object itself. This characteristic was common of the more simple configurations.

Significant portions of the source tube were removed from of the plot in order to get a closer view at the most important aspects of the impulse response where the primary reflections are isolated into a window for training and testing purposes.

In order to create training database, ten examples of each scattering junction type were isolated, identified manually, and then stored. Typically, it is advantageous to have as large of a training database as possible with all training types of an equal amount. It was impossible to broaden the database in this study due to the available tube resources. It would have been beneficial to increase each training set by thirty to define each type more definitively. The scattering junctions in the training database consisted of tubes with diameters of .63 cm and 1.27 cm. The tubes in the testing portion of this study were .95 cm in diameter. It was important that the training and testing junction were of different diameters to confirm that the algorithm can identify the same type of scattering junction, while the cross-sectional areas of the tubes being compared are distinctly different.

<sup>1</sup> For  $x$  repetitions, the signal-to-noise ratio increases by a factor of  $\sqrt{x}$

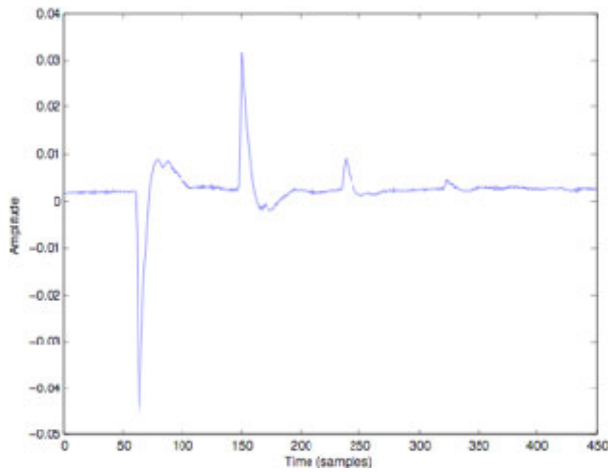


Fig. 2 Impulse response of a closed tube

### 3 Cavity Reconstruction

#### 3.1 Peak-Picking

A peak-picking algorithm was devised to select the appropriate reflections of the test object. Because the source tube is approximately 6.57 m long and the distance  $l_2$  is nearly half the length of the source tube, there are 863 samples between the front of the test object and possible source contamination. That means that any peaks that occur in the impulse response between sample 856 and 1727 must be directly related to the test object itself. Once a reflection is collected, the cause of reflection will be diagnosed during the scattering junction identification process.

The pertinent reflections are obtained by setting a reliable threshold. In the event of a more complex reflection with multiple peaks above the designate threshold, the algorithm selects the greatest peak that occurs in the related sequence of peaks. As a result, no test object segments used in this study are shorter than 24 cm (31 samples). This helps avoid reflection contamination, which would greatly complicate the peak picking and identification processes.

The identified peaks are then stored into a 20-sample window for scattering junction identification. The maximum peak was positioned at the sixth sample of its particular window with the 5 samples previous to the maximum peak to the left and the 14 samples that occurred subsequent samples to the right. The window was arranged in this matter to emphasize the unique idiosyncrasies of the signal following its prominent peak, which were found to have greater evidence of the type of junction at that location. The five samples in the window that occurred before the peak were included to capture the slope that lead to the resulting reflection. The values of each sample were divided by the absolute value of the maximum peak for normalization across the entire database. This provided certainty that the nearest neighbors that border the test reflection do so because of a similar contour, rather than merely sharing similar amplitudes.

Other [6] APR studies utilized duct theory to explain what the contour of each reflection signifies. Duct theory estimates the reflection coefficient that results from a change in cross-sectional area. This relationship is defined as the area ratio,  $a = S_2 / S_1$  for the cross-sectional area of

the first section compared to the second section's cross-sectional area. This ratio can be used to find the magnitude ratio  $M$ . Both  $M$  and  $a$  are defined by the equation s:

$$M = (1 - a) / (1 + a)$$

and (2)

$$a = (1 - M) / (1 + M)$$

Because of these equations, it is apparent that if the cross-sectional area ( $a$ ) increase from segment one to segment two, that the magnitude ratio will be negative. This means that a downward peak will signify an increase in  $a$  and an upward peak will correspond to a decrease in  $a$ .

#### 3.2 Scattering Junction Identification

In this study, scattering junction identification is achieved by means of computer-learning methods. This means that a significant portion of each type of scattering junction is stored in a database and a smaller collection will be used for testing. The computer-learning method utilized for this study was K nearest neighbor. K nearest neighbor (k-NN) is a rather simple algorithm that is a type of instance-based learning, known also as lazy learning.

The K nearest neighbor method was chosen for this particular study due to its quick training phase, which is characteristic of most lazy learning methods. Each training sample is stored as a vector in a multidimensional space. Each vector is given a user-defined classification based on that should be grouped based on similar features, meaning that the time-domain contour of each scattering junction should appear similar to its contemporaries. A successfully defined feature will consist of similarly placed values in the multidimensional space that are separate from a different defined feature. When a query is made, the algorithm looks for the  $k$  closest datasets. The dataset that is being tested will be defined as most prevalent classification amongst the  $k$  closest vectors. If  $k$  were set to three and two of the neighbors were T-intersections and the others was an L-intersection, the scattering junction being tested would be classified as a T-intersection regardless of which junction was the closest in the multi-dimensional space.

Each stored reflection is isolated via the peak-picking algorithm described earlier and then sequentially defined via the k-NN algorithm. An exception to this process occurs when a reflection is classified as a T-intersection. When this occurs, a separate function identifies the next two peaks that are above the threshold as wings. A different peak picking strategy must be implemented for T-intersections, as the reflections that return from wings will likely cohabitate the same peak window.

All of the identified scattering junctions and the segmental distances of the cavity are then placed into a reconstruction algorithm that labels where scattering junctions occur in the test object. The only means for identifying a reflection as point of termination of the tube or of a cross-sectional increase/decrease is during the peak picking process. The reflection of the final segment of a tube tends to be of much greater amplitude than reflections that arrive after the source-to-test object junction. If there is reflection stored type, then the peak is stored is considered the end of the test

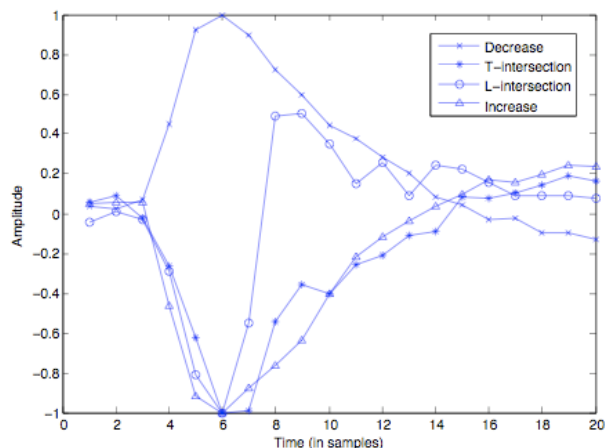


Fig. 3 Scattering Junction Comparisons

object. If there is another peak of common type stored after after the peak and it is labelled as a junction of common the present peak, then it is a common increase/decrease instead. However, it is important to note that both of these types are one in the same; the distinction is only made to better illustrate the test object itself upon reconstruction.

### 3.3 Segment Length

Because sound propagates consistently in air, the delay between each reflection correlates to the length of each portion of the test cavity before the next scattering junction. While each reflection denotes the entrance or termination of a segment, the distance from peak to peak is twice that of the actual length of the tube. This is due to the doubled travel time of the pulse, as the pulse must travel the entire length of the tube before being reflected. Finding the corresponding lengths of each segment is a straightforward task. After obtaining the reflections via the peak-picking algorithm the segment length identifier must work in combination with the scattering junction identification algorithm. In the event of a T-intersection identification, the last two peaks are subtracted from the third to last to correctly identify the proper distance from the intersection. Once the distance between the peaks is found, it is possible can find the length of each tube segment by:

$$L = (c S) / (2 fs) \quad (3)$$

Where  $S$  is the peak-to-peak sample duration,  $fs$  is the sampling rate, and  $c$  is the speed of sound.

## 4 Results

### 4.1 Length Accuracy

Table 1 displays the segment length reconstruction results. The two rows detailing the length deviations are represented in percentage from the actual. Each column represents a particular segment of each cavity being tested. For instance, segment 3b represents the second segment of the third test configuration. A configuration with three segments features a T-intersection. Each column represents a single segment of a particular test cavity. Based on this table it is clear that the lengths were defined with consistency. The estimate that was furthest off (2c) was a 47 cm tube, which is only 2.8 cm off of the actual length. The lengths of the segments ranged from 33 to 47 cm.

All scattering junctions in the 10 test configurations were accurately defined, meaning that all 20 instances in which the junction identification algorithm was employed were successful. During preliminary testing, there was concern whether a cross-sectional increase and T-intersection would be confused, as they are the two most similar contours. Based on our results, it is clear that the identification method was able to distinguish the two.

		Test Segments									
		1	2a	2b	2c	3a	3b	4a	4b	5a	5b
Length		.5	1.5	4	6	1.5	4	1.5	2	2	3
Deviation											
		6	7a	7b	7c	8a	8b	9a	9b	10a	10b
Length		2.5	1.5	5	4	1.5	5	3	2.5	4	4
Deviation											

Table 1 Segment Length

### 4.2 Identification Accuracy

Table 1 details a portion of the junction identification phase of testing. The leftmost column corresponds to the type of scattering junction that was to be identified. The letter next to the test number refers to what kind scattering junction occurs at the end of that segment; I means common increase, D means common decrease, L means L-intersection, and T means T-intersection. Each column is a based on the number of nearest  $k$ 's used. A \* means that the reflection was correctly identified as its actual scattering junction.. An i or t represents a junction that was incorrectly defined as a common increase or T-intersection, respectively.

Based on Table 2, accuracy of identification differs depending on the number of  $k$  neighbors included. It appears that three of the five types of scattering junctions (closed, decrease, and L-intersection) have a distinct and consistent contour resulting in many of the training types sharing the same multidimensional space closely with junctions of the same type. These three types are consistently identified correctly over the course of testing. However, it appears that the T-intersection and cross-sectional increase junctions are identified incorrectly when the amount of  $k$  nearest neighbors is not chosen wisely. This means that the reflection contours of T-intersections and cross-sectional increases are the most similar. Identification was quite accurate when  $k$  was between three and eight. When the number of  $k$ 's is quite large, as is the case when  $k$  is 10, the amount of  $k$ 's is nearly 25% percent of the entire training database, which is not an optimal  $k$  value in such a small training database.

## 5 Conclusions

The results found in this study show that computer-learning methods can be utilized to predict the dimensions of an acoustic space. Scattering junctions can be identified based on their unique reflectivity obtained from an impulse response. Also, the lengths of each segment can be found with regularity.

After confirming the methods presented in this study, it would be beneficial to find if this method could predict larger acoustical spaces where sound does not propagate as a plane waves. The intension of this study was to create a

K Nearest Neighbors												
Test Junction Identification		1	2	3	4	5	6	7	8	9	10	
	C	*	*	*	*	*	*	*	*	*	*	*
	L	*	*	*	*	*	*	*	*	*	*	
	T	I	I	*	*	*	*	*	*	*	*	
	I	*	*	*	*	*	*	*	*	T	T	
	D	*	*	*	*	*	*	*	*	*	*	

Table 2 Junction Identification

foundational method that can learn new features based on an appropriate amount of training no matter the complexity of the scattering junction's contour. As long as there is a consistent feature that can be witnessed across all instances, the algorithm can be taught to effectively identify its occurrence in other instances. In future works, it would be worth investigating various computer-learning methods in order to optimize results.

There are a few improvements that could be done for future works. In addition to the improvements discussed in [7], it could be of interest to find the optimal window size and position during the peak-picking process. Redundant data that is common in all scattering junctions should be eliminated to further separate all junction types in the multi-dimensional space.

## 6 Acknowledgements

This work was supported by a grant from the New York University Challenge Fund.

## 7 References

[1] Sharp D. B. and Campbell D. M. (1997). Leak detection in pipes using acoustic pulse reflectometry. *Acustica* **83**(3): 560-566.

[2] Ware J. A. and Aki K. (1969). Continuous and discrete inverse-scattering problems in a stratified elastic medium. 1 plane waves at normal incidence. *JASA* **45**(4): 911-921.

[3] Sondhi M. M. and Gopinath B. (1971). Determination of vocal-tract shape from impulse response at the lips. *J. Acoust. Soc. Am.* **49**(6): 1867-1873.

[4] Sondhi, M. M. (1981). Acoustical Inverse Problem for the Cochlea. *J. Acoust. Soc. Am.* **69**(2): 500-504.

[5] Carneal, J., Johnson, M E., and Batton, B. (2006). Acoustic reflectometry for determination of waveguide geometry. In *Active 2006*.

[6] Smyth, T. and Abel, J. (2006). Observing the effects of waveguide model elements in acoustic tube measurements. In *Meeting of the Acoustical Society of America*.

[7] Kestian. A. and Roginska, A. (2008). Junction Identification Using Acoustic Reflectometry. In the 124th AES Convention. Amsterdam.

[8] Sharp D. B. (1996). Acoustic pulse reflectometry for the measurement of musical wind instruments. *PhD Thesis*, The University of Edinburgh.